Summary

Electronics represents a corner stone for our modern technology. With the recent development of nanotechnology, people eventually became able to access the adequate length scale to closely investigate the spins and the wide interest and large prospects of using the electrons spin degree of freedom in new generation electronic devices have lead to a vibrant field dubbed spintronics.

In this work, we present experiments in the field of spintronics that combine two very promising materials: single wall carbon nanotubes (SWCNTs) and palladium nickel (PdNi), a tunable ferromagnet, with the purpose to manipulate the electronic spin both in the classical and in the quantum regime. Carbon nanotubes (CNTs) are carbon cylinders of a few nanometers in diameter and up to several millimeters in length. They were discovered by Sumio Iijima in 1991 [1] and they have attracted a lot of interest because of their exceptional electronic and mechanical properties. CNTs have been applied as FETs in logic circuits, and have been also proposed for other electronics applications. More recently, also spin injection and transport in CNTs came under intense scrutiny. The combination of high charge mobility, negligible spin-orbit coupling and weak hyperfine interaction holds the promise of very long spin relaxation times.

Pd_xNi_{100-x} (where x represents the atomic concentration, in percent) alloy also attracted considerable attention as ferromagnetic electrodes in carbon based spin valves. Its excellent contact properties on carbon nanotubes (CNT), lead to low resistance contacts (transparent) [2], while its ferromagnetic behavior provides the means for spin injection. Surprisingly in the case of CNTs a tunneling barrier between the PdNi and the CNT itself seems not to be an indispensable ingredient for spin injection. In fact the anisotropy of the alloy plays an important role since the successful demonstration of spin injection is based on the observation of a giant magnetoresistance (GMR) effect, determined by the relative orientation between the magnetization of the ferromagnetic electrodes. In carbon-based spin-valve devices the planar arrangement of the system complicates the realization of non-collinear magnetizations, and the ability to control the magnetization direction with respect to the plane of the electrode which is an essential factor in the evolution of the system. For this, a good knowledge of the magnetic properties of such ferromagnetic alloys when lithographically patterned into narrow electrodes.

Manipulating spin or magnetization requires to apply a torque via a real or an effective magnetic field. Not so long ago it was shown that spin polarized current is another possibility to achieve the same results thanks to the spin transfer torque phenomenon [5]. So far, the spin transfer torque has been intensely studied in systems (nanopillars [6], magnetic stripes [7] etc) exhibiting a classical, essentially diffusive, transport mechanism. In this context, the question to ask is: what happens when these classical conductors are replaced by quantum ones such as nanowires or quantum dots. The immediate interest in such systems, beside the fundamental phenomenology involved is a new generation of electronic devices where the spin transfer torque dominates over heating and/or Oersted field effects.

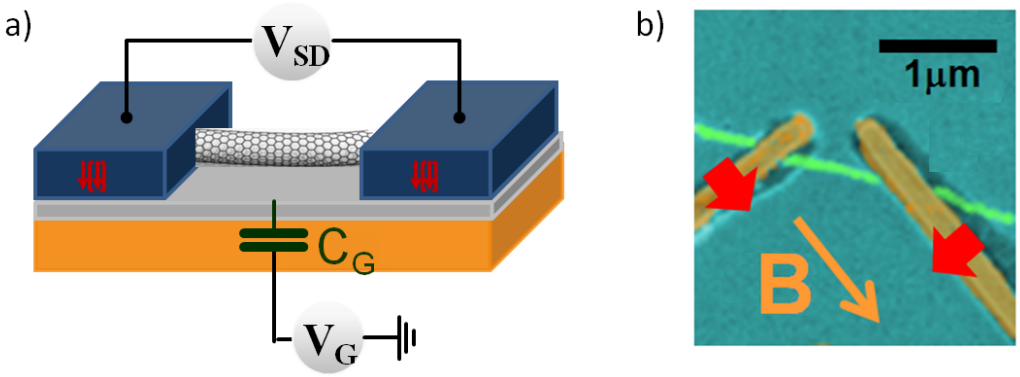

Figure 1: *(a) Schematic view of a CNT based quantum dot: two metallic leads (source and drain) are evaporated on the CNT; the nanotube is capacitively connected to a gate voltage while a source-drain tension is used to vary the chemical potential of the electrodes; (b) SEM image of a typical sample in false colors. The red arrows indicate the direction of the magnetizations. A back gate electrode (not visible) is used to tune the energy levels of the device. As shown by the orange arrow, the external B-field is applied along one of the easy axis of the two PdNi strips. A bias voltage (not visible) is used to tune the electrochemical potentials of the electrodes.*

The control which is generally offered when scaling down to nanometric dimensions allows one to achieve new functionalities with high potential, as it is the case of the spin field effect transistors [8], [9]. So far, results of such a high potential have been demonstrated only for collinear geometry-based systems, where spin transport can be described using a single quantization axis. Still, magnetoelectronics devices exploiting actively the electronic spin, meaning a total control over classical or quantum spin rotations have not been achieved so far.

Here we implement a quantum dot connected to two non-collinear ferromagnetic leads forming an angle of $\theta = \pi/2$, schematically presented in fig. 1, (a). The device we propose acts like a spin-valve device. A finite tunneling magnetoresistance effect

is to be expected. in fig. 1, (b) one can see a SEM image of a typical sample in false colors. The red arrows indicate the direction of the magnetization of the two leads. A back gate electrode (which is not emphasized in the image, see fig. 1, (a)) is used to tune the energy levels of the device. As shown by the orange arrow, the external magnetic field, B, is applied along the easy axis of one of the PdNi stripes.

Main results

PdNi anisotropy

For a better understanding of the magnetic switchings taking place in such a device and also for optimizing its electronic properties, a detailed understanding of the magnetic characteristics of Pd_xNi_{100-x}, alloy becomes crucial. During this work we studied PdNi alloy nanostripes by means of extraordinary Hall effect measurements on lithographically patterned crosses (see fig. 2) by varying the chemical composition of the alloy, its thickness and the capping films used to impede oxidation.

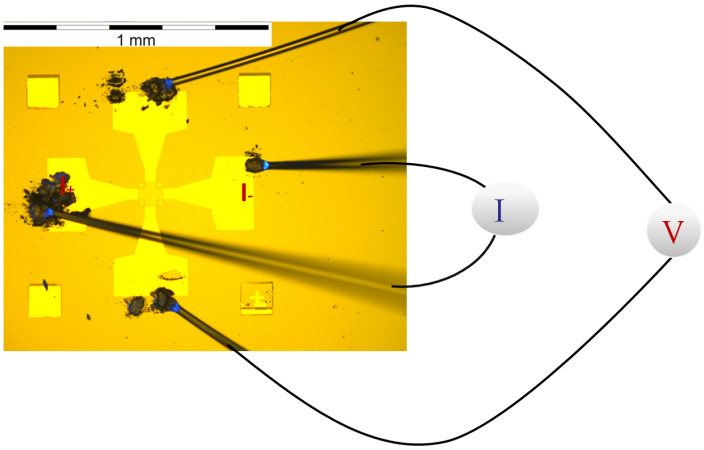

Figure 2: *Optical image of a typical Hall cross; the PdNi crosses are connected to Au pads further contacted using a microbonding machine to the sample holder; the principle of a 4-points electrical measurement is exposed in the image: we measure the voltage difference V while applying an electrical current between the I_+ and I_- terminals.*

The results presented here were measured on samples having 40 μm in width and a length of 100 μm. We investigated also nanometric sized samples with 300 nm in width and 2 μm in length. The thickness of PdNi varied between 5 and 15 nm. Capping layers of aluminium, palladium and samples without capping were probed. All samples were fabricated on a Si substrate and structured via electron beam lithography. The deposition of the thin films was done using evaporation techniques. Gold (Au) leads are attached to the PdNi crosses as contact pads for electrical measurements; small

Au crosses are used to align the patterns during the various steps of lithography. The study focused on $Pd_{20}Ni_{80}$ and $Pd_{90}Ni_{10}$.

A first question we wanted to anwser to regards the influence that the proportion of Pd in PdNi alloy has on the anisotropy of ones' samples. For that, both, $Pd_{90}Ni_{10}$ and $Pd_{20}Ni_{80}$ were investigated. Measurements performed on $Pd_{20}Ni_{80}$ for temperatures between 10 K and 140 K in a field sweeping between -9 T and 9 T show a saturation field between 100 and 200 mT that increases with the increase of the temperature and a lack of remanent magnetization. This testifies for the in-plane magnetization alignment of the sample, even at the lowest temperatures.

The hysteretic curves for $Pd_{90}Ni_{10}$, in the same interval of temperatures, show an evolution from in-plane to out-of-plane magnetization at around 60 K. An increase in the coercive field with the decrease of temperature is emphasized.

An important aspect when considering the transition from $Pd_{20}Ni_{80}$ to $Pd_{90}Ni_{10}$ is lower magnetization of the later alloy (average atomic moment $\mu = 0.6$ B for $Pd_{20}Ni_{80}$ while $\mu = 0.25$ B for $Pd_{90}Ni_{10}$ as Fischer et al reported [**?**]), thus a smaller demagnetization energy for the $Pd_{90}Ni_{10}$. On the other hand, magnetostriction initially increases with the increase of the Pd percentage in the compound. So, when analyzing $Pd_{90}Ni_{10}$ we have a smaller demagnetization while more anisotropy in the system thus a bigger chance to observe an out-of-plane magnetization.

For $Pd_{20}Ni_{80}$, this experiment is a first at low temperature and results show that the magnetization remains in plane even at $T = 10$ K This translates into a small stray magnetic field exerted by the material which is very helpful in constructing small size spin valve devices with ferromagnetic leads. Indeed, the result is very helpful for the second part of this work, the one concentrated on quantum spin valve effect since an in plane magnetization translates into a small stray magnetic field exerted by the electrodes.

Also a comparison between the Curie temperature of the two alloys: about 120 K for $Pd_{90}Ni_{10}$ while for $Pd_{20}Ni_{80}$ this is well above room temperature (reported at 600 K by Ferrando et al [10]) offer an obvious facility in the case of $Pd_{20}Ni_{80}$ to use further room temperature techniques for a more thorough investigation. Following these results, in our CNT based spin devices, we used a Ni-rich alloy for the electrodes connecting the CNT, due to the in-plane orientation of the magnetization that produces a small stray field.

Extraordinary Hall measurements confirm previous experiments [3], [4] that showed a preferential direction of high aspect ratio PdNi contact strips, with a magnetically easy axis transverse to the strip orientation. Furthermore, we provide experimental

proof for the model proposed by Chauleau et al who interpreted this magnetically easy axis, transversal to the strip orientation as a consequence of the stress/strain relaxion at the strip edges. While a perpendicular component magnetization effect was also recorded for the core of the stripe, according to Chauleau et al the edges remain transverse.

Further measurements show that geometry, thickness and the choice of capping layer used to protect the PdNi against oxidation, are all key parameters when choosing the right characteristics for a spin-based device. Measurements done on nanometric sized Hall crosses show a out-of-plane component of the magnetization at small temperatures (below 40 K), but less than in the case of the micrometric samples. This is due to due to the stress relaxation at the edges that becomes important, in relative terms, in such small devices.

Non-collinear magneto-electronics/Spin dependent transport in quantum dots

An important factor in quantum dots physics, due to the spatial confinement of electrons, is the (Coulomb) electron-electron interaction. The tunneling of electrons from the ferromagnetic electrodes to the island is strongly influenced by the Coulomb charging energy of the QD. Tunneling of an electron into such an island increases the electrostatic energy of the island by the charging energy $E_C = e^2/2C$, where e represents the electronic charge and C is the total capacitance of the QD.

When speaking about electron tunneling we need to consider the transparency of the contacts between the CNT and metallic leads. In samples with low contact transparency, a pronounced Coulomb blockade is observed, where single-electron conductance peaks are separated by broad valleys of vanishing conductance. To observe Coulomb blockade regime, thus discrete charges inside the QD, one needs that the transmission events between the leads and the island are much smaller than one.

In the case of a more transparent contact between the island and the leads, we can speak about a Fabry-Perot transport regime which is the electronic analog to the Fabry-Perot interferometer. In this regime, the electronic interactions can be neglected.

Measurements presented in this section were performed on CNTs connected to ferromagnetic electrodes, of nominal composition $Pd_{30}Ni_{70}$, 45 nm thick, covered with 5 nm of Pd. The conductance measurements are done using a standard lock-in detection technique. Each magnetoresistance plot was obtained by averaging 4 times single curves, all displaying a hysteresis switching. The external magnetic field is applied along the direction of one of the electrodes and thus perpendicular to the second one to ensure the maximum effect differences while swept between $\pm 0.4\ T$.

Coulomb blockade transport regime

Transport measurements revealed a Coulomb blockade transport regime, confirmed by a color scale differential conductance map of the device (see fig 3) as a function of the source-drain bias V_{SD} and the gate voltage V_g for the transport spectroscopy over a wide range of voltages. The color scale plot displays specific Coulomb diamonds characteristic to the spectroscopy of a quantum dot. The mean level spacing variate with the gate region: from smaller in the gate region displayed ($< 1\ meV$), to substantially larger (about 3 meV) for more positive values of the gate.

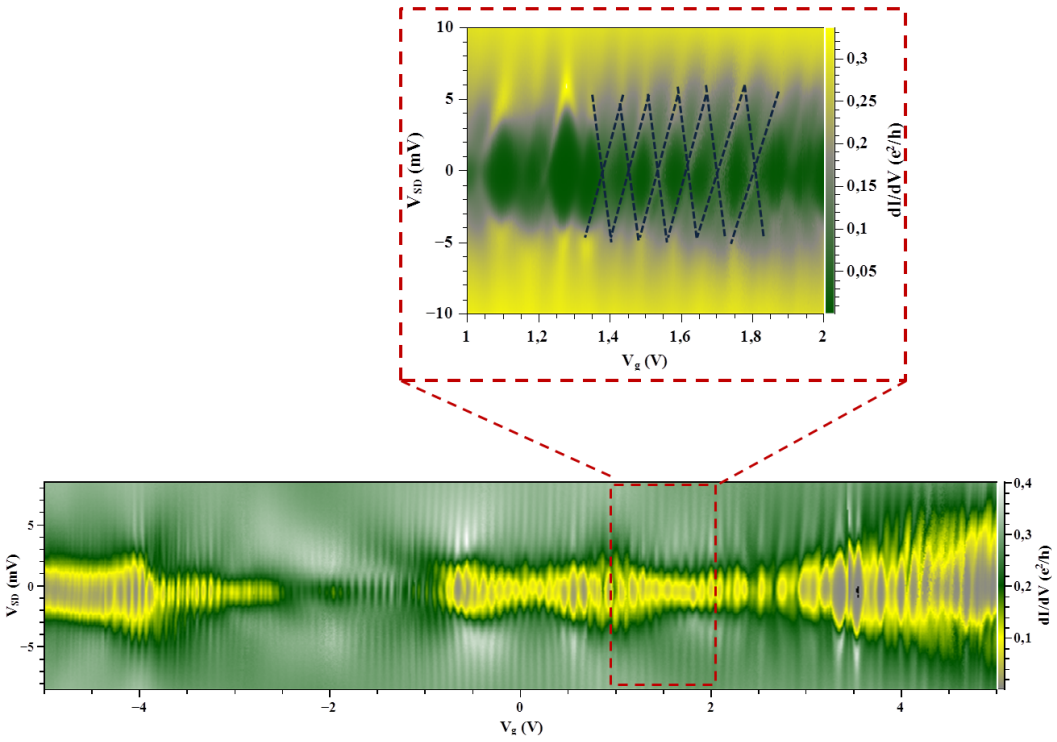

Figure 3: *Color scale differential conductance spectroscopy of the device as a function of gate voltage, V_g (over a wide range), and source-drain bias, V_{SD}. Characteristic Coulomb diamonds are displayed. Experimental temperature is* 1.8 K.

The sample was further tested in both linear regime (in the absence of a source-drain voltage) and non-linear one. In linear regime, results show a typical TMR signal when placed under the sweeping field, behavior specific for a spin-valve device. The hysteretic switchings are symmetric with respect to the 0 external magnetic field and correspond to modifications in the relative magnetization of the electrodes.

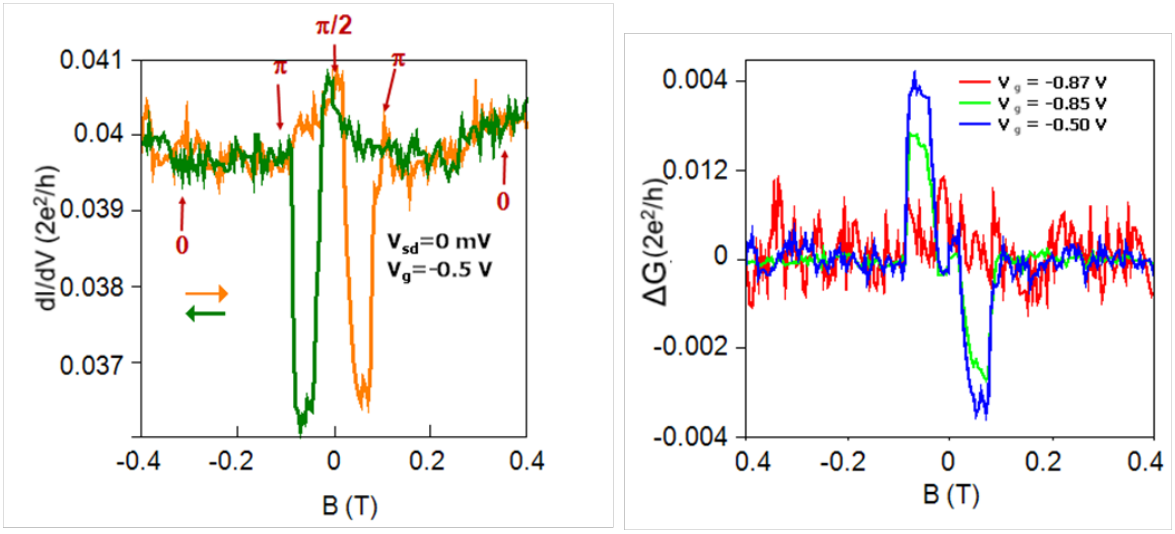

Figure 4: *Gate effect on magneto-resistance* (a) *Single magnetoresistance curve for* $V_{sd} = 0\ mV$ *and* $V_g = -0.5\ V$. *The orange curve corresponds to increasing magnetic field* (G_{trace}). *The green curve corresponds to decreasing magnetic fields* $(G_{retrace})$. (b) *Variations of the jumps magnitude* $(\Delta G = G_{trace} - G_{retrace})$ *were observed for different values of* V_g .

Plots of the conductance, dI/dV, as a function of V_g show a clear high conductance for negative gate voltages. In fig. 4, (a), it is displayed a typical hysteretic swich registrated for a gate voltage: $V_g = -0.5\ V$ where is indicated also the evolution of the relative angle between the magnetizations of the two ferromagnetic electrodes. The first switch can be translated as the return of the magnetization in one of the leads leading to the relative degree between the two magnetization of $\theta = \pi$. The second switching event is attributed to a modification of the angle θ from π to 0. If one defines the amplitude of the hysteresis, ΔG, as the difference in conductance upon increasing the external magnetic field, G_{trace}, and decreasing the external magnetic field, $G_{retrace}$, then as it can be seen in fig. 4, (b), for different gate voltages ($V_g = -0.87\ V$, $V_g = -0.85\ V$ $V_g = -0.5\ V$) the jumps magnitude changes.

The TMR signal oscillates with the gate voltage due to the quantum behavior of the nanotube connected to the leads. The oscillations of the TMR stem from quantum interferences phenomena as well as interactions taking place inside the device.

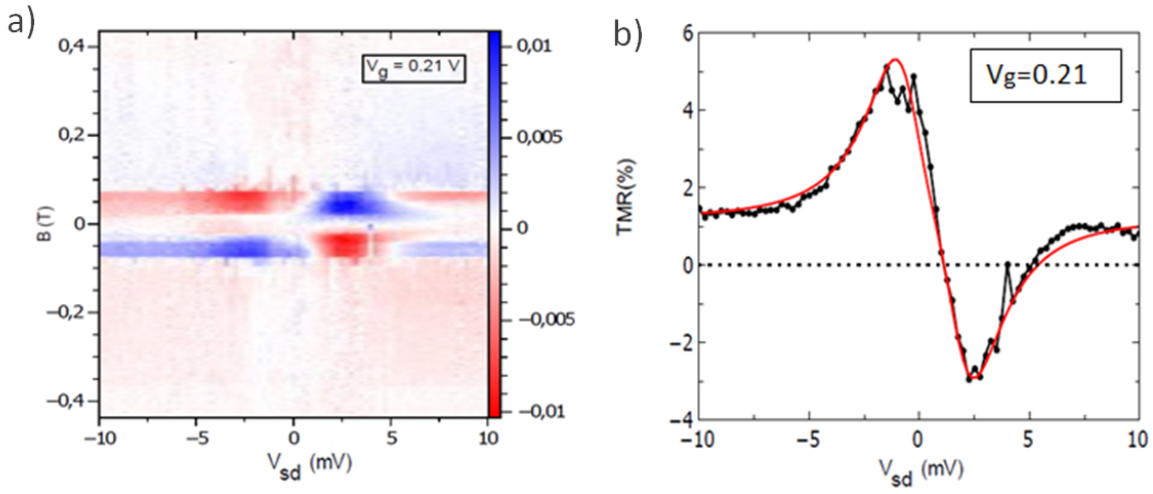

Figure 5: *(a) Wide range gate voltage variation of the spin signal* $\Delta G = G_{trace} - G_{retrace}$ *in color scale as a function of the magnetic field,B, and the source-drain* V_{SD}*.* $V_g = 0.21\ V$*; (b) Black line - linear conductance measured simultaneously with the spin signal, red line - prediction of the proposed model with appropiate parameters.*

In the non-linear regime the hysteresis signal (the spin signal $\Delta G = G_{trace} - G_{retrace}$) measured on a wide source-drain voltage range as a function of the magnetic field, B, for a gate voltage $V_g = 0.21\ V$ (displayed in fig. 5, (a)) it can be identified a change of sign as the bias changes from positive to negative values. Also the TMR displays a nearly anti-symmetric behavior around the 0 magnetic field point (see fig. 5, (b)). Measurements done for different values of the gate voltage account for the non triviality of this behavior. Comparison of the expermental data with calculations supports the hypothesis of an interplay between spin accumulation phenomena which tends to force the spin inside the dot to follow the symmetry of the current and spin relaxation that acts against it, a precession of the spin inside the QD (see schematics in fig. 6) is taking place.

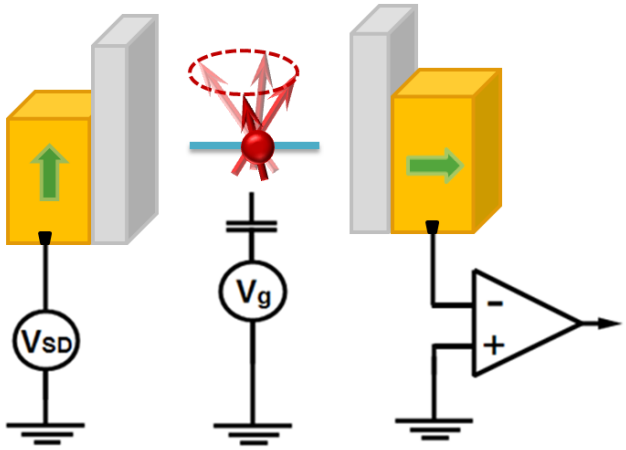

Figure 6: *Illustration of the phenomenological behavior of the device. A single active energy level carries a single spin which can take in principle any direction since it is controlled by non-collinear electrodes. A concurential behavior between spin accumulation phenomena which tends to force the spin inside the dot to follow the symmetry of the current and spin relaxation that acts against it, determine a precession of the spin inside the QD.*

Fabry-Perot transport regime

Colorscale plots of the conductance as a measure of the source-drain and gate voltages confirm the chessboard like pattern specific to the Fabry-Perot physics. The spacing between the centers of two adjacent rhombs gives access to the spacing of the energy levels inside the quantum dot (QD) which is, experimentallly, determined by, L, the length of the nanotube: $\Delta E = hv_F/L$. In our case the spacing between rhombs is 5 mV as highlighted in fig. , (a), using orange dashed lines and it is consistent with the lithographically defined length of the nanotube which is about 600 nm.

Measurements performed in the linear regime were used to characterize the spin transport in the absence of a source-drain voltage. The signal registered has a hysteretic evolution, with the switchings indicating modifications in the magnetization of the PdNi leads. Measurements done on a large interval of gate voltages show consistent variations in the jumps magnitude up to 4 %.

A striking result obtained here in presented in fig. 7, (b). A similar hysteretic curve was obtained in out of equilibrium transport regime for multiple gate voltages values. The hysteretic signal shows magnetization reversal in the electrodes taking place before the external magnetic field applied changes sign. The phenomena was studied both when the field increases and decreases.

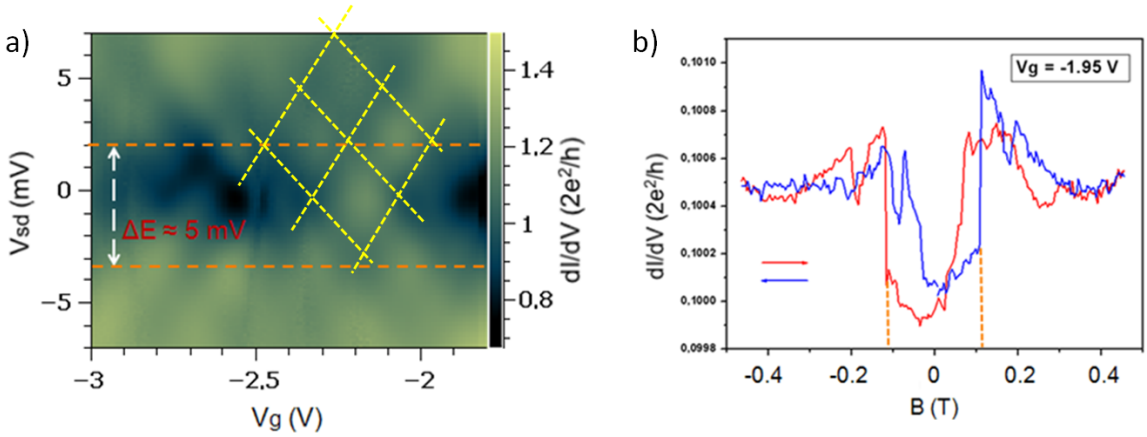

Figure 7: (*a*) *Color scale differential conductance spectroscopy of the device over a wide range of source-drain bias* V_{SD} *and gate voltage. Characteristic chessboard patters - highlighted by the yellow dotted line, specific to Fabry-Perot physics. Experimental temperature is* 1.8 K. (*b*) *Single magnetoresistance curve for* $V_g = -1.95\ V$. *Magnetization reversal before the external field changes sign.*

While it is too early for a final conclusion on the nature of this result, this preliminary work may suggest a transfer torque that "helps" the external applied field to switch the magnetization inside the two ferromagnetic PdNi leads. This result is even more important since it represents a first in such type of structure. Nevertheless more investigations need to be pursued to present a final picture of the phenomenology involved.

Bibliography

[1] S. Iijima. *Helical microtubules of graphitic carbon.* Nature, 354, pages 56 - 58 (1991).

[2] Y. Matsuda, W.-Q. Deng, III W. A. Goddard *Contacts resistance for "end-contacted" metal-graphene and metal-nanotube interfaces from quantum mechanics.* J. Phys Chem, 114 (2010)

[3] J.-Y. Chauleau, B.J. McMorran, R. Belkhou, N. Bergeard, T.O. Mentes, M. A. Nino, A. Locatelli, J. Unguris, S. Rohart, J. Miltat, A. Thiaville. *On the magnetization textures in NiPd nanostructures.* Phys. Rev. B, B 84, 094416 (2011).

[4] C. Feuillet-Palma, T. Delattre, P. Morfin, J.-M. Berroir, G. Feve, D. C. Glattli, B. Placais, A. Cottet, and T. Kontos. *Conserved spin and orbital phase along carbon nanotubes connected with multiple ferromagnetic contacts.* Phys. Rev. B, B 81, 115414 (2010).

[5] A. Brataas, G. E. W. Bauer, P. J. Kelly. *Non-collinear Magnetoelectronics.* (2007).

[6] E. B. Myers, D. C. Ralph, J. A. Katine, R. N. Louie, R. A. Buhrman. *Current Induced Switching of Domains in Magnetic Multilayer Devices.* Science, 285, 5429, pages 867-870, 5429.867 (1999).

[7] J.-Y. Chauleau, R. Weil, A. Thiaville, J. Miltat. *Magnetic domain walls displacement : automotion vs. spin-transfer torque.* Phys. Rev. B, 82, 214414 (2010).

[8] S. Sahoo and T. Kontos, J. Furer, C. Hoffman, M. Graber, A. Cottet, C. Schronenberger. *Electric field control of spin transport.* Nature Physiscs, 1:99 (2005).

[9] J. Paaske, J.R. Hauptman and P.E. Lindelof. *Electric-field-controlled spin reversal in a quantum dot with ferromagnetic contacts.* Nature Physics, 4, 373-376 (2008).

[10] W. A. Ferrando, R. Segnan, A. I. Schindlerl. Phys. Rev. B, B5, 4657 (1972).